Synthetic and Systems Biotechnology 10 (2025) 237–246

Contents lists available at ScienceDirect

Synthetic and Systems Biotechnology

journal homepage: www.keaipublishing.com/en/journals/synthetic-and-systems-biotechnology

Original Research Article

Coordinated regulation of two LacI family regulators, GvmR and GvmR2, on guvermectin production in *Streptomyces caniferus*

Haoran Shi [a,b,1], Jiabin Wang [a,b,1], Shanshan Li [b], Chongxi Liu [a], Lei Li [a,b], Zhuoxu Dong [a,b], Lan Ye [a,b], Xiangjing Wang [a], Yanyan Zhang [b,*], Wensheng Xiang [a,b,**]

[a] Key Laboratory of Agricultural Microbiology of Heilongjiang Province, Northeast Agricultural University, Harbin, 150030, China
[b] State Key Laboratory for Biology of Plant Diseases and Insect Pests, Institute of Plant Protection, Chinese Academy of Agricultural Sciences, Beijing, 100193, China

ARTICLE INFO

Keywords:
Guvermectin
Biopesticide
Regulatory mechanisms
Functional interaction
High-yield strategy

ABSTRACT

Guvermectin, a purine nucleoside natural product produced by the genus *Streptomyces*, has recently been registered as a new biopesticide to boost rice yield. Despite its economic and agricultural significance, the regulatory mechanisms of guvermectin biosynthesis remain essentially unknown, hindering industrial production and widespread agricultural application. Here, we examined the roles of two LacI family regulators, *gvmR* and *gvmR2*, located within and adjacent to the guvermectin biosynthesis cluster, respectively, in guvermectin production in *Streptomyces caniferus* NEAU6. GvmR activated the expression of the guvermectin cluster by binding to the promoters of *gvmR*, *gvmA*, and *O1*, while GvmR2 repressed the guvermectin cluster via competitive binding to promoters containing GvmR-binding sites, specifically, a 14-bp palindromic sequences: 5′-RTCATWCGYATGAY-3′ (R = G/A, W = A/T, Y = T/C). Moreover, GvmR indirectly activates the expression of *gvmR2* while GvmR2 feedback inhibits *gvmR* transcription, suggesting a functional interaction between the two regulators for coordinating guvermectin production. Overexpression of *gvmR* via the T7 RNA polymerase-T7 promoter system in the *gvmR2* mutant significantly elevated guvermectin production by 125 % (from 631 mg L^{-1} to 1422 mg L^{-1}), compared to the parental strain NEAU6. This suggested that combinatorial manipulation of *gvmR* and *gvmR2* is useful for improving guvermectin production. These findings enrich our knowledge of the regulatory network for guvermectin biosynthesis, and offer key targets and effective strategies for high-titer guvermectin production.

1. Introduction

Guvermectin is a purine nucleoside natural product (NP) that is produced by several *Streptomyces* species, including *Streptomyces angustmyceticus*, *Streptomyces decoyicus*, and *Streptomyces caniferus* [1–4]. This product possesses potent plant growth-promotion activities. In a study involving 28 rice varieties, soaking seed in guvermectin significantly promoted root and coleoptile growth, increased tillering, shortened the maturation period, and increased yield by 6.2–19.6 %. Notably, this yield-increasing effect surpassed that of commercial growth-promoting biopesticides, including cytokinins (CKs), brassinosteroids (BRs), and gibberellin-auxin-BR mixtures [4,5]. Due to its superior effects on rice growth and yield, guvermectin was registered in 2021 as a new biochemical pesticide in China (registration number PD20212929) and is considered a valuable asset for increasing global crop yields.

To meet the anticipated agricultural demand for guvermectin, it will be necessary to optimize production of this NP. Over the past four years, the biosynthetic gene cluster (BGC) controlling guvermectin production has been identified in *S. angustmyceticus* NBRC 3934, *S. decoyicus* NRRL 2666, and *S. caniferus* NEAU6 [6–8]. The guvermectin gene clusters in these three strains share strong similarities. Each contains nine genes: six key biosynthetic enzymes genes (*gvmA*, *gvmB*, *gvmC*, *gvmD*, *gvmE*, and *gvmF*), one regulatory gene (*gvmR*), and two major facilitator superfamily (MFS) transporter genes (*gvmT1* and *gvmT2*). In-depth genetic and biochemical studies have previously been conducted to delineate

Peer review under responsibility of KeAi Communications Co., Ltd.
* Corresponding author.
** Corresponding author. Key Laboratory of Agricultural Microbiology of Heilongjiang Province, Northeast Agricultural University, Harbin, 150030, China.
E-mail addresses: yyzhang@ippcaas.cn (Y. Zhang), xiangwensheng@neau.edu.cn (W. Xiang).
[1] These authors contributed equally to this work.

https://doi.org/10.1016/j.synbio.2024.11.001
Received 18 September 2024; Received in revised form 1 November 2024; Accepted 3 November 2024
Available online 9 November 2024

the guvermectin biosynthetic pathway, which proceeds through multiple steps utilizing the six biosynthetic enzymes with D-fructose 6-phosphate and ATP as precursors [6,8]. The MFS transporters GvmT1 and GvmT2 are hypothesized to export guvermectin from the cytoplasm to the external environment, but the specific functions of the two transporter genes remain unknown [7]. Inactivation of *gvmR* leads to almost no production of guvermectin, suggesting an essential role of *gvmR* in guvermectin biosynthesis [7]. However, the corresponding regulatory mechanism has not yet been demonstrated.

NPs derived from *Streptomyces* are often produced at relatively low levels due to stringent control of their biosynthesis through sophisticated intracellular regulatory networks [9]. DNA-binding transcriptional regulators are primary components of such regulatory networks, playing essential roles in determining NP production and final titer [10,11]. Cluster-situated regulators (CSRs) often determine the production levels of a cognate NP through direct control of BGC gene expression [9]. BGC expression is also controlled by upstream signal transduction pathways mediated by global or pleiotropic regulators. These signal inputs are coordinated in part by regulatory cascades and in part by convergence of regulators on the promoters of common targets, particularly CSRs [9]. CSRs therefore serve as integral, efficient switches for expression of specific local BGCs, and CSR-type regulator-based genetic engineering approaches have been widely applied in NP discovery and overproduction [12,13].

In the present study, we investigated the regulatory mechanisms of guvermectin biosynthesis in *S. caniferus* NEAU6 by characterizing the cluster-situated regulatory gene *gvmR* and the cluster-adjacent regulatory gene *gvmR2*. The differential regulatory mechanisms of GvmR and GvmR2 in modulating guvermectin biosynthesis and the cross-regulatory relationships between them were uncovered. Leveraging these insights, we tuned the expression of *gvmR* in the *gvmR2* mutant, which led to a synergistic increase in guvermectin production to 1.25-fold higher than the parental strain NEAU6.

2. Materials and methods

2.1. Strains, plasmids, primers, and culture conditions

The strains and plasmids utilized in this work were listed in Table S1, and primers used were summarized in Table S2. *Streptomyces caniferus* NEAU6 is a wild-type guvermectin producer. ΔgvmR is a *gvmR* inactivation mutant generated from *S. caniferus* NEAU6 [8]. *Streptomyces coelicolor* M1146 was used for β-glucuronidase (GUS) assays [14]. *Escherichia coli* JM109 was used as a general host for propagating plasmids. *E. coli* ET12567 (pUZ8002) was used for transferring DNA from *E. coli* to *Streptomyces* via conjugation [15]. *E. coli* BL21 (DE3) was used to express GST-tagged GvmR and GvmR2. The *E. coli-Streptomyces* shuttle plasmid pKC1139, which contains a temperature-sensitive origin of replication derived from pSG5, was used to construct the *gvmR2* deletion plasmid [16]. Plasmids pIJ10500 and pSET152, which are capable of integrating into the *Streptomyces* chromosome via site-specific recombination at the phage ΦC31 or ΦBT1 attachment site (*attB*), respectively [16,17], were used to construct recombinant plasmids for gene complementation, overexpression and GUS assays. *S. caniferus* NEAU6 and its derivatives were cultured at 28 °C on YMS agar medium for spore collection [18]. Seed medium (2 % sucrose, 2 % maltdextrin, 6 % soybean powder, and 0.3 % $CaCO_3$, pH 7.0) and fermentation medium (1 % sucrose, 6 % maltdextrin, 4 % soybean powder, and 0.4 % $CaCO_3$, pH 7.2) were used for NEAU6 vegetative mycelium preparation and guvermectin production, respectively. AS-1 medium was prepared for GUS assays as described previously [19]. LB medium was used to cultivate *E. coli* strains. MS medium was used for interspecies conjugation from *E. coli* to *Streptomyces* [15].

2.2. Gene disruption, complementation and overexpression

For the complementation of *gvmR* in ΔgvmR, two plasmids pIJ10500:gvmR and pIJ10500:P_{hrdB}gvmR were constructed. To construct pIJ10500:gvmR, a 1681-bp fragment containing the open reading frame (ORF) and the upstream region of *gvmR* was amplified by PCR from *S. caniferus* NEAU6 genomic DNA using primers CNgvmR-F/R. This fragment was then inserted into the *Spe*I/*Xho*I sites of pIJ10500 by Gibson assembly to generate pIJ10500:gvmR. To construct pIJ10500:P_{hrdB}gvmR, the *hrdB* promoter and the *gvmR* ORF were individually amplified from the genomic DNAs of *S. coelicolor* and *S. caniferus* NEAU6 with primer pairs PhrdB-F/R and CHgvmR-F/R. The two obtained fragments and the *Spe*I/*Xho*I digested pIJ10500 were ligated together through Gibson assembly to generate pIJ10500:P_{hrdB}gvmR. The two complementation plasmids verified by PCR and sequencing were individually introduced into ΔgvmR by conjugal transfer to generate the complementation strains ΔgvmR/gvmR and ΔgvmR/P_{hrdB}gvmR.

To construct the *gvmR2* deletion mutant, two homologous fragments gvmR-L (2485 bp) and gvmR-R (2187 bp) flanking the *gvmR* gene were amplified by primers DR2UP-F/R and DR2DN-F/R using the genomic DNA of *S. caniferus* NEAU6 as template, respectively. The two fragments were inserted into the *Hin*dIII/*Xba*I sites of pKC1139 through Gibson assembly to obtain pKC1139:ΔgvmR2. pKC1139:ΔgvmR2 was then introduced into NEAU6 via conjugation to generate the *gvmR2* deletion mutant (ΔgvmR2).

For the complementation of *gvmR2* in ΔgvmR2, a 1599-bp fragment containing the *gvmR2* ORF and its upstream region was amplified using primers CNgvmR2-F/R and NEAU6 genomic DNA, and inserted into the *Eco*RI/*Xba*I sites of pSET152 by Gibson assembly to generate pSET152:gvmR2. pSET152:gvmR2 was introduced into ΔgvmR2 by conjugation to obtain the complementary strain ΔgvmR2/gvmR2. For the overexpression of *gvmR2* in NEAU6, a 1147-bp fragment containing the ORF of *gvmR2* was amplified with primers OHgvmR2-F/R, and inserted into the *Pac*I/*Xba*I sites of pSET152:P_{hrdB} through Gibson assembly to generate pSET152:P_{hrdB}gvmR2. This plasmid was introduced into NEAU6 to generate *gvmR2* overexpression strain NEAU6/P_{hrdB}gvmR2.

For the overexpression of *gvmR*, three recombinant plasmids pSET152:gvmR, pSET152:2gvmR, and pSET152:pHT7gvmR were constructed using the *gvmR* native promoter and the strong constitutive T7 RNA polymerase-T7 promoter system [20]. To construct pSET152:gvmR, a 1681-bp fragment containing the *gvmR* coding region and its upstream regulatory region was amplified using primers ONgvmR-F/R and inserted into the *Eco*RI/*Xba*I sites of pSET152 to generate pSET152:gvmR; to construct pSET152:2gvmR, two fragments (1587 bp and 1588 bp) containing *gvmR* ORF and its upstream region were amplified using primes ON1R–F/R and ON2R–F/R, and the two fragments were ligated to the *Eco*RI/*Xba*I sites of pSET152 to obtain pSET152:2gvmR. To construct pSET152:pHT7gvmR, The *hrdB* promoter and the coding region of T7 RNA polymerase (T7 RNApol) were individually amplified from the genomic DNA of *S. coelicolor* and the plasmid pACTe with primer pairs hrdB-pF/R and T7RNApol-F/R [20]. The obtained fragments P_{hrdB} and T7 RNApol were ligated into the sites of *Xba*I and *Bam*HI in pSET152 to give pHT7RNApol, in which T7 RNA polymerase is driven by the *hrdB* promoter. The T7 promoter and terminator regions (PT7 and T7ter) were amplified with primer pairs T7-F/R and T7ter-F/R using pET23b (+) as template, respectively. The *gvmR* coding region with its 5' UTR (UNemR) was obtained by PCR from genomic DNA of *S. caniferus* NEAU6 with primers OT7R–F/R. The plasmid pHT7RNApol was digested with *Eco*RI and assembled with PT7, T7ter and UGvmR to obtain the overexpression plasmid pSET152:pHT7gvmR, which was introduced into *S. caniferus* NEAU6 by intergenic conjugation to obtain the overexpression strain NEAU6/pHT7gvmR.

2.3. HPLC analysis of guvermectin

For extraction of guvermectin, 0.4 ml whole cell fermentation broth

was treated by ultrasound for 1 h, followed by centrifugation at 12000 rpm for 10 min. The resulting supernatant was used for HPLC analysis. HPLC analysis was carried out by Agilent 1260 II system with an Sq-C18 column (Zorbax, 4.6 × 250 mm, 5 μm) at a flow rate of 0.8 ml/min with 90 % solvent A and 10 % solvent B in 30 min (Solvent A: ddH_2O; Solvent B: CH_3CN) and detected at 260 nm.

2.4. RNA preparation, RT-PCR, and quantitative real-time RT-PCR

Total RNAs were extracted from NEAU6 and its derivatives fermented for various time points. RNA isolation, examination of RNA quality and quantity, cDNA synthesis, RT-PCR and qRT-PCR were performed as previous report [21].

2.5. Expression and purification of GvmR and GvmR2

To construct GvmR expression plasmid, the coding region of *gvmR* was amplified from the genome of NEAU6 using primer pair GEXgvmR-F/R. The PCR product was cloned into the *Bam*HI/*Xho*I digested pGEX-4T-1 to obtain pGEX-4T-1:gvmR. The construction process of GvmR2 expression plasmid pGEX-4T-1:gvmR2 was similar to that of constructing pGEX-4T-1:gvmR. The coding region of *gvmR2* was amplified from the genomic DNA of NEAU6 using primer pair GEXgvmR2-F/R and subsequently inserted into the *Bam*HI/*Xho*I digested pGEX-4T-1 to obtain pGEX-4T-1:gvmR2. The overexpression and purification processes were the same as described previously [22].

2.6. Electrophoretic mobility shift assays (EMSAs)

EMSAs were performed as reported previously [21]. The promoter probes were amplified from the genomic DNA of NEAU6 by PCR with primer pairs listed in Table S2.

2.7. Site-directed mutagenesis of GvmR and GvmR2 binding sequences

To evaluate the specificity of GvmR on its binding sequence, the bidirectional promoter region $P_{R\text{-}A}$ was inserted into the *Eco*RV digested pBluescript KS(+) to generate pBlu:$P_{R\text{-}A}$. Three fragments containing mutated $P_{R\text{-}A}$ were amplified using pBlu:$P_{R\text{-}A}$ as template by primer pairs *Nhe*I-F/R, *Nde*I-F/R and *Nhe*I-F/*Nde*I-R, respectively, which were self-ligated, generating mutant plasmids pBlu:$P_{R\text{-}A}$-M1 pBlu:$P_{R\text{-}A}$-M2 and pBlu:$P_{R\text{-}A}$-M3. These three plasmids were further used as templates separately to amplify mutant probes $P_{R\text{-}A}$-M1, $P_{R\text{-}A}$-M2 and $P_{R\text{-}A}$-M1 by primer pair gvmRA-pF/R. The binding activities of GvmR or GvmR2 to the three probes were subsequently determined by EMSAs.

2.8. GUS assays

GusA activities were measured as described previously [23,24]. To determine the potential promoter activities of *gvmT1*, *gvmT2*, *gvmE* and *gvmF*, the corresponding promoters of them were obtained from the NEAU6 genomic DNA by PCR with primer pairs gvmT1GUSA-pF/R, gvmT2GUSA-pF/R, gvmEGUSA-pF/R, gvmFGUSA-pF/R, respectively (Table S2), which were cloned into the upstream of *gusA* (encoding β-glucuronidase) reporter based on pSET152 by Gibson assembly, generating plasmids pSET152:P_{T1}gusA, pSET152:P_{T2}gusA, pSET152:$P_E$gusA, pSET152:$P_F$gusA. These four plasmids together with the control plasmid pSET152:gusA were introduced into M1146 by conjugal transfer to generate derivatives M1146/gusA, M1146/P_{T1}gusA, M1146/P_{T2}gusA, M1146/$P_E$gusA, and M1146/$P_F$gusA, respectively.

To determine the importance of the 14-bp palindromic sequences for GvmR regulatory activity *in vivo*, the promoter region of *gvmA* (P_A) and the corresponding mutant probes (P_A-M1, P_A-M2 and P_A-M3) were PCR amplified using pBlu:$P_{R\text{-}A}$, pBlu:$P_{R\text{-}A}$-M1, pBlu:$P_{R\text{-}A}$-M2 and pBlu:$P_{R\text{-}A}$-M3 as templates by primers PgvmA-XF/R, respectively. Each of these four fragments, the promoterless *gusA* and P_{hrdB} activated *gvmR* were assembled into the *Pvu*I/*Eco*RV digested pSET152:hyg, generating plasmids pSyg:$P_A$gusA::P_{hrdB}gvmR, pSyg:P_A-M1gusA::P_{hrdB}gvmR, pSyg:P_A-M2gusA::P_{hrdB}gvmR, and pSyg:P_A-M3gusA::P_{hrdB}gvmR. In addition, P_A and the promoterless *gusA* were inserted into the *Xba*I/*Eco*RV digested pSET152:hyg, generating the control plasmid pSyg:$P_A$gusA. These plasmids were then introduced into ΔgvmR by conjugation.

To determine the regulatory effects of GvmR2 on *gvmR* and *gvmA*, the promoter regions of *gvmR* and *gvmA* were PCR amplified using primers gvmRGUSA-pF/R and gvmAGUSA-pF/R. Each of the two fragments and the promoterless *gusA* were assembled into the *Pvu*I/*Xba*I sites of pSET152, generating pSET152:$P_R$gusA and pSET152:$P_A$gusA. Then the P_{hrdB} controlled *gvmR2* were assembled into the *Bam*HI/*Eco*RI digested pSET152:$P_R$gusA and pSET152:$P_A$gusA, generating two new plasmids pSET152:P_{hrdB}gvmR2::$P_R$gusA and pSET152:P_{hrdB}gvmR2::$P_A$gusA. These four plasmids were then introduced into *S. coelicolor* M1146 by conjugation.

2.9. Measurement of cell growth

Cell growth was measured using a simplified diphenylamine colorimetric method established previously [25].

2.10. Statistical analysis

All experiments were performed at three biological replicates. Data are presented as averages of three replicates. Significance was analyzed by Student's *t*-test, and the significance is presented as follows, $*P < 0.05$, $**P < 0.01$.

2.11. Bioinformatics analysis

The sequence alignment and domains of potential protein-coding sequences (CDSs) were documented by publicly available databases and their application tools, including Pfam (http://www.pfam.xfam.org/) and SMART (http://www.smart.embl-heidelberg.de/). Motif-based sequence analysis tools were created by MEME (https://meme-suite.org/meme/index.html).

3. Results

3.1. Bioinformatics analysis and transcriptional profiles of gvmR and gvmR2

gvmR is located upstream of the operon containing the six essential guvermectin biosynthetic enzyme genes (*gvmA–F*) in the opposite orientation (Fig. 1A). Analysis of the corresponding protein sequence showed that *gvmR* encoded a LacI-family regulatory protein of 339 amino acids (aa) in length, including an N-terminal LacI-type HTH motif and a C-terminal sensor (Peripla_BP_3) domain, which can respond to small molecules such as sugars, sugar phosphates, sugar acids, and purines [26]. Approximately 8 kb upstream of the *gvmT1* locus (Fig. 1A), *gvmR2* (*scn1129*) encodes a LacI-family regulator of 334 aa in length, which shares 51.7 % identity with GvmR. To characterize the correlation between these two regulators and guvermectin biosynthesis, we first analyzed their transcriptional profiles during guvermectin production. Total RNAs were extracted from *S. caniferus* NEAU6 cultures after cultivation for 0.5, 1, 2, 3, 5, and 8 days in a guvermectin fermentation medium. The transcription of *gvmR* and *gvmR2* was assessed by quantitative real-time RT-PCR (qRT-PCR). Transcription of *gvmR* was low at 0.5 day and increased gradually, whereas that of *gvmR2* peaked at 1 day and decreased slightly thereafter (Fig. 1B). These data indicated that the transcriptional patterns of the two genes are distinct, suggesting their differential regulatory roles in *S. caniferus* NEAU6.

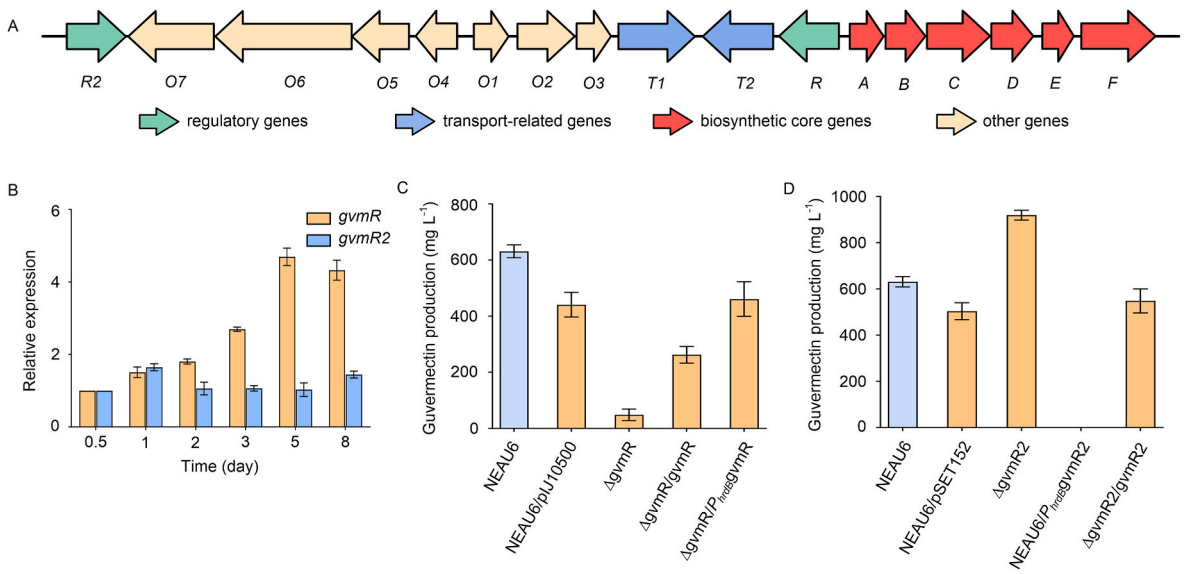

Fig. 1. Effect of *gvmR* and *gvmR2* on guvermectin production. (A) Genetic organization of the guvermectin biosynthetic gene cluster and its upstream genes. Each arrow indicates a separate open reading frame (ORF) and orientation of transcription. (B) qRT-PCR analysis of *gvmR* and *gvmR2* in the parental strain NEAU6. RNA samples were isolated from cultures at 0.5, 1, 2, 3, 5 and 8 days. Gene expression levels are normalized to the NEAU6 value at 0.5 day, which is set to 1. (C) Comparative guvermectin production in NEAU6, NEAU6/pIJ10500, ΔgvmR and two complementation strains (ΔgvmR/gvmR and ΔgvmR/P_{hrdB}gvmR). (D) Comparative guvermectin production in strains NEAU6, NEAU6/pSET152, ΔgvmR2, ΔgvmR2/gvmR2 and NEAU6/P_{hrdB}gvmR2.

3.2. Functions of gvmR and gvmR2 in guvermectin production

To determine the *in vivo* roles of *gvmR* and *gvmR2*, genetic experiments, including gene knockout, gene complementation and overexpression, were performed. Our previous work showed that *gvmR* inactivation caused substantial decrease in guvermectin production [8]. To further verify the function of *gvmR*, a native copy of *gvmR* or a copy driven by the constitutive promoter P_{hrdB} in the integrative plasmid pIJ10500 was introduced into the *gvmR* inactivation mutant (ΔgvmR). This generated the complementation strains ΔgvmR/gvmR and ΔgvmR/P_{hrdB}gvmR (Fig. S1), respectively. The empty vector pIJ10500 was introduced into NEAU6 to form the control strain NEAU6/-pIJ10500. The two complementary strains, the two control strains (NEAU6 and NEAU6/pIJ10500), and ΔgvmR were cultured in fermentation medium for 8 days, then guvermectin production was quantified with HPLC (Fig. 1C). Consistent with previous findings, Δ*gvmR* produced only trace amounts of guvermectin. Conversely, complementation of ΔgvmR with *gvmR* restored production to hundreds of milligrams per liter. Notably, introduction of the empty vector pIJ10500 had an adverse effect on guvermectin production, decreasing the titer by 30 % compared to the NEAU6 control (Fig. 1C). Production in the complementation strains was thus compared to the empty vector control strain NEAU6/pIJ10500, which produced 441 mg L^{-1} guvermectin. In comparison, ΔgvmR/gvmR and ΔgvmR/P_{hrdB}gvmR showed 60 % (263 mg L^{-1}) and 105 % (461 mg L^{-1}) restoration of guvermectin production, respectively (Fig. 1C). These data demonstrated a positive role of GvmR in guvermectin production.

To assess the involvement of *gvmR2* in guvermectin production, a *gvmR2* deletion mutant (ΔgvmR2) was created via homologous recombination. In ΔgvmR2, a 693-bp fragment within the *gvmR2* ORF was deleted (Fig. S1). Subsequent fermentation and HPLC analysis revealed a 45.6 % increase in guvermectin production (from 631 mg L^{-1} to 919 mg L^{-1}) in ΔgvmR2 compared to the NEAU6 strain. Additionally, two recombinant plasmids, pSET152:gvmR2 and pSET152:P_{hrdB}gvmR2, were constructed using the integrative vector pSET152. In pSET152:gvmR2, *gvmR2* was expressed under its native promoter, while in pSET152:P_{hrdB}gvmR2, it was controlled by the constitutive P_{hrdB}. pSET152:gvmR2 was introduced into ΔgvmR2 to generate the complemented strain ΔgvmR2/gvmR2; pSET152:P_{hrdB}gvmR2 and the empty vector pSET152 were introduced into NEAU6 to obtain the overexpression strain NEAU6/P_{hrdB}gvmR2 and the control strain NEAU6/pSET152. Compared to NEAU6, guvermectin production decreased by 25 % in NEAU6/pSET152, indicating a negative impact of the pSET152 integration into the ΦC31 *attB* site of *S. caniferus* NEAU6 (Fig. 1D). The titer of guvermectin in ΔgvmR2/gvmR2 was comparable to that of NEAU6/pSET152, whereas NEAU6/P_{hrdB}gvmR2 exhibited no detectable guvermectin production (Fig. 1D). These results demonstrated that GvmR2 acts as a negative regulator of guvermectin production and that the empty plasmid pSET152 adversely affects the phenotype of NEAU6.

3.3. GvmR activates, and GvmR2 represses guvermectin BGC expression

gvmR is a CSR gene within the guvermectin BGC, and *gvmR2* is a regulatory gene situated adjacent to the guvermectin BGC. These two genes may modulate guvermectin production by controlling the expression levels of some guvermectin BGC genes. We first determined the effect of GvmR on expression of these genes, total RNAs were isolated from mycelia of NEAU6 and ΔgvmR cells cultured for 2 and 5 days, then qRT-PCR was performed to assess the expression of guvermectin BGC genes. Compared to NEAU6, the expression of *gvmR*, the exporter gene *gvmT1*, and the representative structural genes (*gvmA*, *gvmD*, *gvmE*, and *gvmF*) was significantly downregulated in ΔgvmR at both time points (Fig. 2A). In contrast, the other exporter gene, *gvmT2*, was slightly upregulated in ΔgvmR (Fig. 2A), this could have been due to insertional inactivation of the *gvmR* open reading frame (ORF) by the apramycin resistance gene *acc3IV* (Fig. S1). Overall, these results indicated that GvmR positively controlled guvermectin production by activating genes in the guvermectin BGC. Moreover, the impact of *gvmR* inactivation on *gvmR2* expression was also examined. The transcription of *gvmR2* decreased significantly in ΔgvmR, indicating that GvmR also positively influences *gvmR2* expression (Fig. 2A).

Subsequently, the effect of GvmR2 on guvermectin BGC expression was assessed by qRT-PCR using RNAs isolated from the mycelia of NEAU6, ΔgvmR2, and NEAU6/P_{hrdB}gvmR2 cultured for 2 and 5 days. The transcriptional levels of all seven BGC genes were significantly higher in ΔgvmR2 than in NEAU6 at 2 days, whereas at 5 days, the transcript levels of two genes (*gvmD* and *gvmE*) were significantly lower in ΔgvmR2 than in NEAU6 (Fig. 2B). In NEAU6/P_{hrdB}gvmR2, the

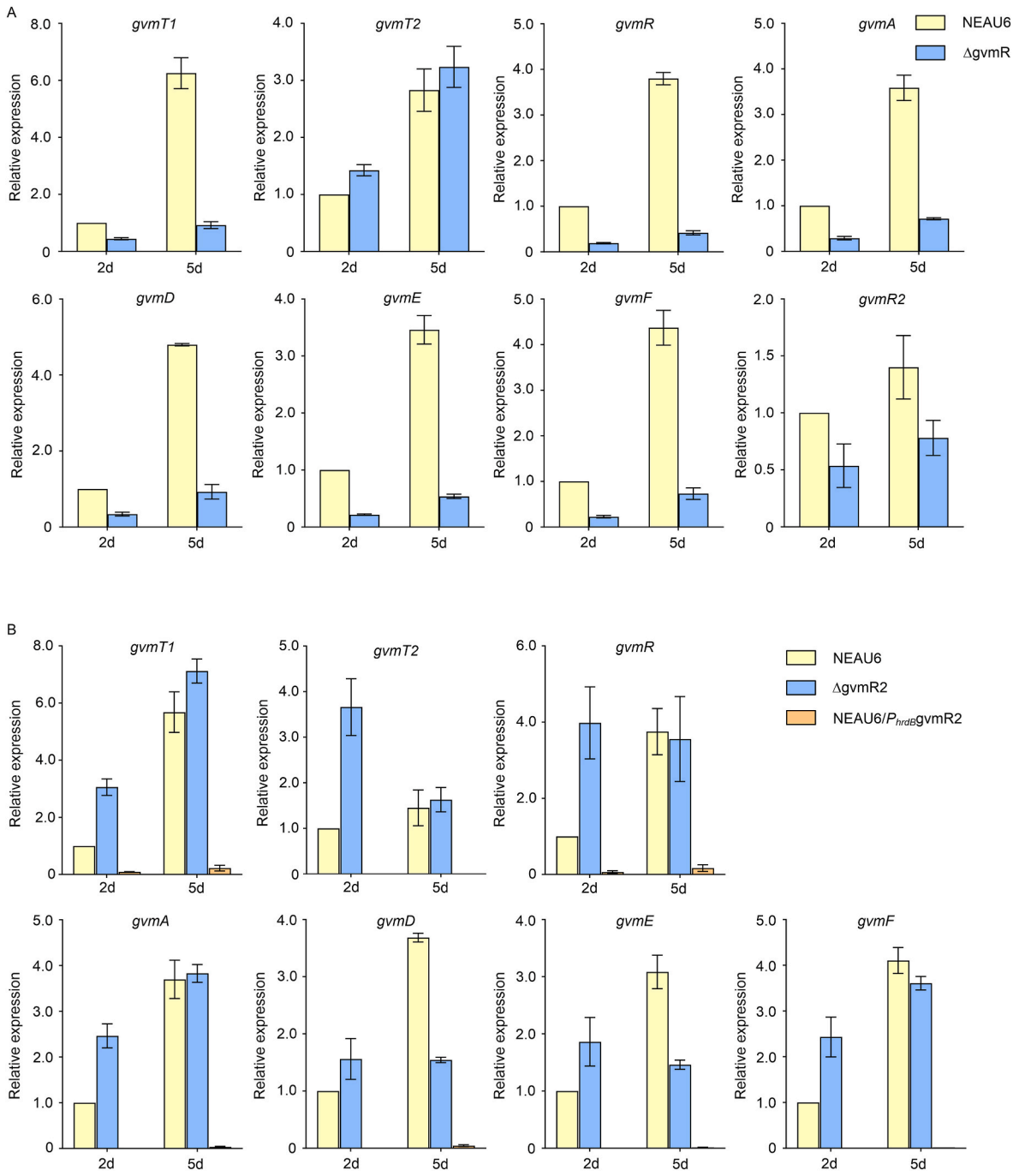

Fig. 2. qRT-PCR analysis to determine the effects of *gvmR* and *gvmR2* on the transcription of guvermectin BGC genes. (A) Transcriptional analysis of guvermectin BGC genes in strains NEAU6 and ΔgvmR. (B) Transcriptional analysis of guvermectin BGC genes in strains NEAU6, ΔgvmR2 and NEAU6/P_{hrdB}gvmR2. RNA samples were isolated from 2- and 5-days cultures. Transcription of each gene was calculated relative to the NEAU6 value on day 2 or day 5, assigned a value of 1. Transcription of 16S rRNA was used as the internal control.

transcripts of these genes were markedly reduced, reaching very low or undetectable levels at both time points (Fig. 2B), indicating that GvmR2 negatively regulates guvermectin production by repressing guvermectin BGC transcription.

3.4. Both GvmR and GvmR2 can binds to the bidirectional gvmR–A and O1 promoters

Identifying the direct targets of GvmR and GvmR2 is important to understand how they control expression of guvermectin BGC genes. We began by analyzing the putative operons and promoter regions within the guvermectin BGC. Sequence analysis suggested that *gvmA–gvmF* and *gvmR-gvmT2* may form polycistronic units, but that *gvmE*, *gvmF*, and *gvmT2* might also have their own promoters. *gvmT1* was located furthest upstream within the guvermectin BGC. The NEAU6 genome sequence revealed the presence of three convergently transcribed genes (*O1*, *O2*, and *O3*) upstream of *gvmT1* (Fig. 3A), suggesting that *gvmT1* may either have independent promoter activity or be controlled by the *O1* promoter.

To confirm our speculation and determine the authentic operons and promoter regions, we conducted RT-PCR-based co-transcription analysis and β-glucuronidase-based GUS assays. For co-transcriptional analysis,

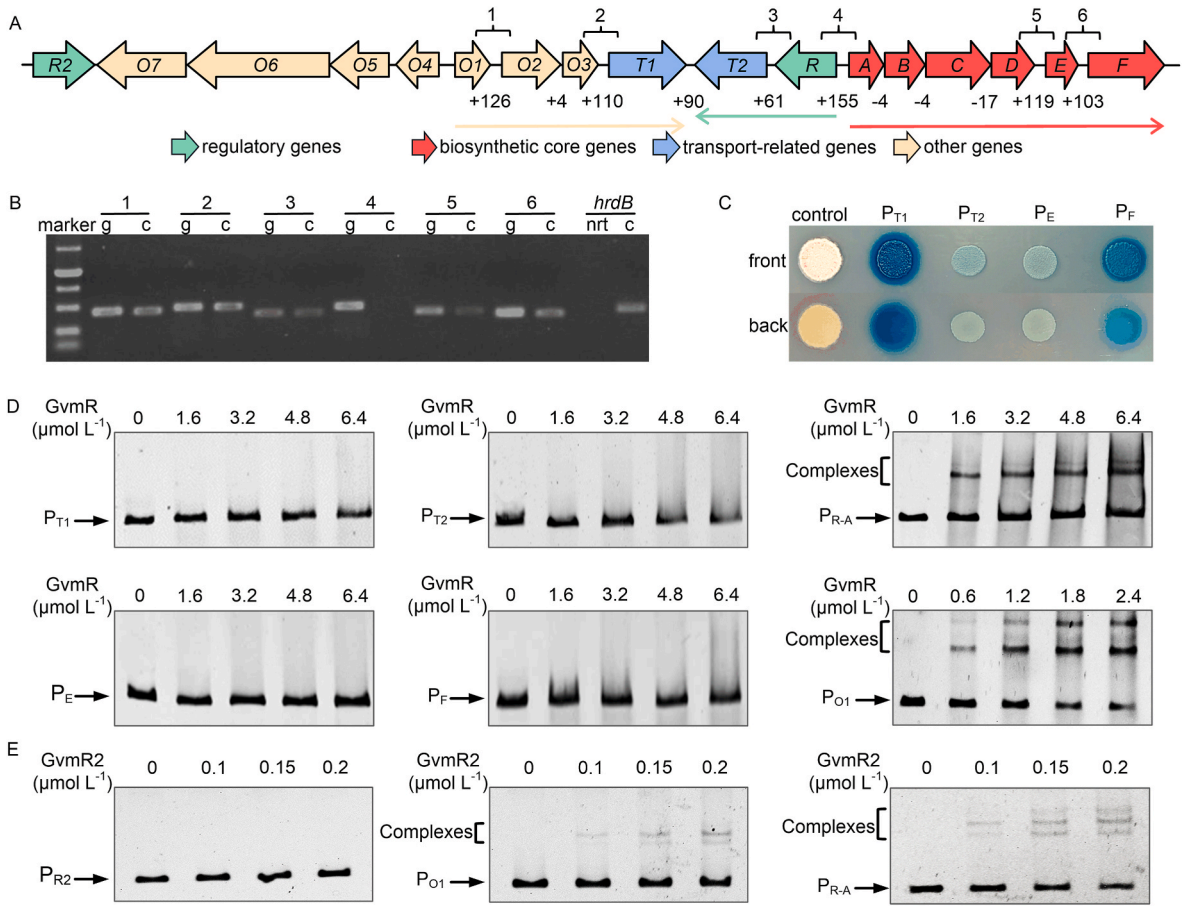

Fig. 3. EMSAs to determine the direct targets of GvmR and GvmR2. (A) The "extended guvermectin BGC", including three additional genes that may have been co-transcribed with *gvmT1*. Intergenic regions labelled 1–6 were analyzed with RT-PCR. The three analyzed operons are indicated with long horizontal arrows in varying colors; the numbers below the guvermectin BGC indicate the distance between adjacent ORFs. (B) Co-transcription analysis of the guvermectin BGC. cDNA was generated from the total RNAs of NEAU6 strain cultured for 2 days. g, genomic DNA. c, cDNA template. nrt, "cDNA" template generated without reverse transcriptase. (C) GUS assays to measure the activities of the native *gvmT1*, *gvmT2*, *gvmE* and *gvmF* promoters. (D) EMSAs to assess interactions between GvmR and its target promoter regions. (E) EMSAs of the interactions between GvmR2 and its target promoter regions.

six primer pairs specific for intergenic regions 1–6 were designed (Fig. 3A–Table S2). RT-PCR was then performed using RNA extracted from the mycelia of NEAU6 fermented for 2 days. As expected, PCR products spanning the intergenic regions of *O1/O2*, *O3/gvmT1*, *gvmT2/gvmR*, *gvmD/gvmE*, and *gvmE/gvmF* were detected (Fig. 3B). This indicated that the nine guvermectin BGC genes (*gvmR*, *gvmT1*, *gvmT2*, and *gvmA–gvmF*) belonged to three polycistronic units: *O1–gvmT1*, *gvmR–gvmT2*, and *gvmA–gvmF*. For GUS assays, the regions upstream of *gvmT1*, *gvmT2*, *gvmE*, and *gvmF* (i.e., the putative promoters P_{T1}, P_{T2}, P_E, and P_F, respectively) were each inserted upstream of the *gusA* (encoding β-glucuronidase) coding region in the pSET152 vector. Subsequently, these constructs together with the control plasmid pSET152:gusA (containing only *gusA* ORF) were introduced into *Streptomyces coelicolor* M1146, respectively. Compared with the pSET152:gusA control strain, which showed no GUS activity, strains containing P_{T1} or P_F had strong GUS activity and those containing P_{T2} or P_E had weak but detectable GUS activity (Fig. 3C). These results suggested that each of the four genes could be controlled not only by upstream polycistronic promoters but also by their own promoters.

The co-transcriptional analysis and GUS assays showed that the extended guvermectin cluster (classified as the guvermectin BGC together with *O1–O3*) contained at least seven promoter regions. These promoter regions together with the *gvmR2* promoter were used for EMSAs with N-terminal GST-tagged GvmR and GvmR2 to identify direct binding targets (Fig. S2). GvmR formed complexes with $P_{R\text{-}A}$ (the bidirectional *gvmR–gvmA* promoter) and P_{O1} (the promoter region of *O1*) (Fig. 3D), while no complexes were detected with the other promoter regions (Fig. 3D and Fig. S3). GvmR2 similarly bound to $P_{R\text{-}A}$ and P_{O1} but did not interact with the other promoters (Fig. 3E and Fig. S3). These results indicated that GvmR activates guvermectin BGC transcription by binding to the *gvmR-gvmA* and *O1* promoter regions, while GvmR2 represses transcription of guvermectin BGC by binding to the same promoter regions. Additionally, GvmR appears to indirectly activate *gvmR2* expression.

Given that $P_{R\text{-}A}$ functions as a bidirectional promoter, the binding of GvmR2 to $P_{R\text{-}A}$ implies that GvmR2 may inhibit the expression of both *gvmR* and *gvmA*, or possibly just one of them. To clarify the specific inhibition mechanism of GvmR2 at this bidirectional promoter, GUS assays were performed. The *gvmR* and *gvmA* promoters were inserted upstream of *gusA* to generate the constructs pSET152:$P_R$gusA and pSET152:$P_A$gusA, respectively. These constructs were introduced into *S. coelicolor* M1146. Additionally, the P_{hrdB} controlled *gvmR2* was assembled into the above two recombinant plasmids to generate pSET152:$P_R$gusA::P_{hrdB}gvmR2 and pSET152:$P_A$gusA::P_{hrdB}gvmR2, respectively, which were also introduced into *S. coelicolor* M1146. GUS activity was assessed in these four strains using agar-based chromogenic assays. GUS activity was readily observed in strains carrying pSET152:$P_R$gusA or pSET152:$P_A$gusA, whereas no activity was detected in strains with pSET152:$P_R$gusA::P_{hrdB}gvmR2 or pSET152:$P_A$gusA::P_{hrdB}gvmR2 (Fig. S4). These findings indicated that GvmR2 inhibits gene expression from both *gvmR* and *gvmA* promoters.

3.5. Confirmation of GvmR and GvmR2 binding sequences

Because LacI/Gal family regulators typically interact with palindromic sequences in target promoter regions [27,28], we searched for such sequences in $P_{R\text{-}A}$ and P_{O1}. Four highly similar 14-bp palindromic sequences were detected in the two promoter regions: sites I and II in $P_{R\text{-}A}$ and sites III and IV in P_{O1} (Fig. 4A). The sequences of sites I and II were identical. As for site III, compared with the sequence of site I, the base at position 7 is "G" instead of "A", and the base at position 7′ is "C" instead of "T" (Fig. 4B); Site IV differed from site III only at position 2, with a corresponding change at position 2' (Fig. 4B).

To determine whether the 14-bp palindromic sequence was essential for the DNA binding activity of GvmR and GvmR2, three mutated DNA probes were generated based on the $P_{R\text{-}A}$ sequence: $P_{R\text{-}A}$-M1, $P_{R\text{-}A}$-M2, and $P_{R\text{-}A}$-M3 (Fig. 4C). In $P_{R\text{-}A}$-M1, site I was replaced by an *Nde*I restriction site; in $P_{R\text{-}A}$-M2, site II was replaced by an *Nhe*I restriction site; and in $P_{R\text{-}A}$-M3, sites I and II were replaced with *Nde*I and *Nhe*I restriction sites, respectively. These mutated DNA probes together with the wild-type $P_{R\text{-}A}$ were then tested in EMSAs with GvmR and GvmR2 (Fig. 4D). Incubation of GvmR with $P_{R\text{-}A}$ resulted in one shifted band at low protein concentrations. At a higher concentration of GvmR (2.4 μM), a new shallow shifted band appeared above the first band. In contrast to $P_{R\text{-}A}$, $P_{R\text{-}A}$-M1 and $P_{R\text{-}A}$-M2 each formed just one band after incubation with 2.4 μM GvmR. Furthermore, $P_{R\text{-}A}$-M3 did not form any complexes with GvmR, suggesting that at least one palindromic sequence was necessary for GvmR binding to $P_{R\text{-}A}$. For the interaction of $P_{R\text{-}A}$ with GvmR2, mutating site I or site II individually did not affect their binding, while double mutation of the two sites resulted in the $P_{R\text{-}A}$ losing its ability to bind to GvmR2 (Fig. 4D), indicating that the palindromic sequences are critical for $P_{R\text{-}A}$ binding with GvmR2.

Next, we selected the regulatory protein GvmR to assess the necessity of these 14-bp palindromic sites for $P_{R\text{-}A}$ promoter activity and further confirm their importance in mediating the control of *gvmA*-oriented gene expression *in vivo*. We designed and prepared a $P_{R\text{-}A}$ promoter probe that was shortened by 142 bp (P_A), which drove gene expression in the direction of *gvmA* (Fig. 5A). Three P_A mutants (P_A-M1, P_A-M2, and P_A-M3) were then derived from $P_{R\text{-}A}$-M1, $P_{R\text{-}A}$-M2, and $P_{R\text{-}A}$-M3, respectively. Each of these four new promoters was inserted into pSET152 upstream of *gusA*, yielding pSET152:$P_A$gusA, pSET152:P_A-M1gusA, pSET152:P_A-M2gusA and pSET152:P_A-M3gusA constructs. *gvmR* controlled by P_{hrdB} was subsequently assembled into the above four recombinant plasmids to generate pSET152:$P_A$gusA::P_{hrdB}gvmR, pSET152:P_A-M1gusA::P_{hrdB}gvmR, pSET152:P_A-M2gusA::P_{hrdB}gvmR and pSET152:P_A-M3gusA::P_{hrdB}gvmR, respectively. These four constructs along with pSET152:$P_A$gusA were introduced into ΔgvmR to generate five new strains ΔgvmR/$P_A$gusA::P_{hrdB}gvmR, ΔgvmR/P_A-M1gusA::

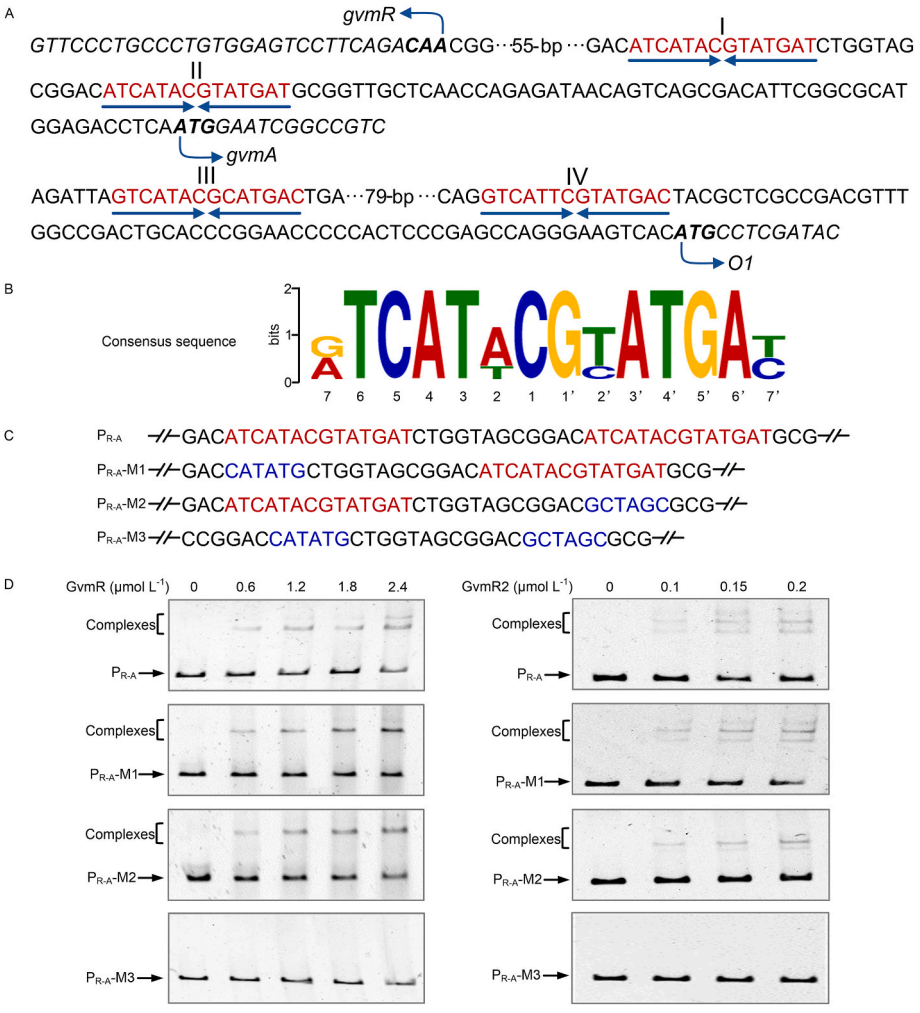

Fig. 4. Determination of GvmR and GvmR2 conservative binding sites. (A) Four similar 14-bp palindromic sequences discovered in the intergenic region between *gvmR* and *gvmA* ($P_{R\text{-}A}$) and in the region upstream of *O1* (P_{O1}). The translation start sites of *gvmR*, *gvmA* and *O1* are indicated with curved arrows. The palindromic sequences are shown in red and marked with dark blue arrows. (B) Conservative sequence analysis of these binding sites. (C) Diagrams showing the mutations made to the two palindromic sequences in $P_{R\text{-}A}$. Substituted nucleotides are indicated in blue. (D) EMSAs showing GvmR and GvmR2 binding to $P_{R\text{-}A}$ and the mutated probes $P_{R\text{-}A}$-M1, $P_{R\text{-}A}$-M2, and $P_{R\text{-}A}$-M3.

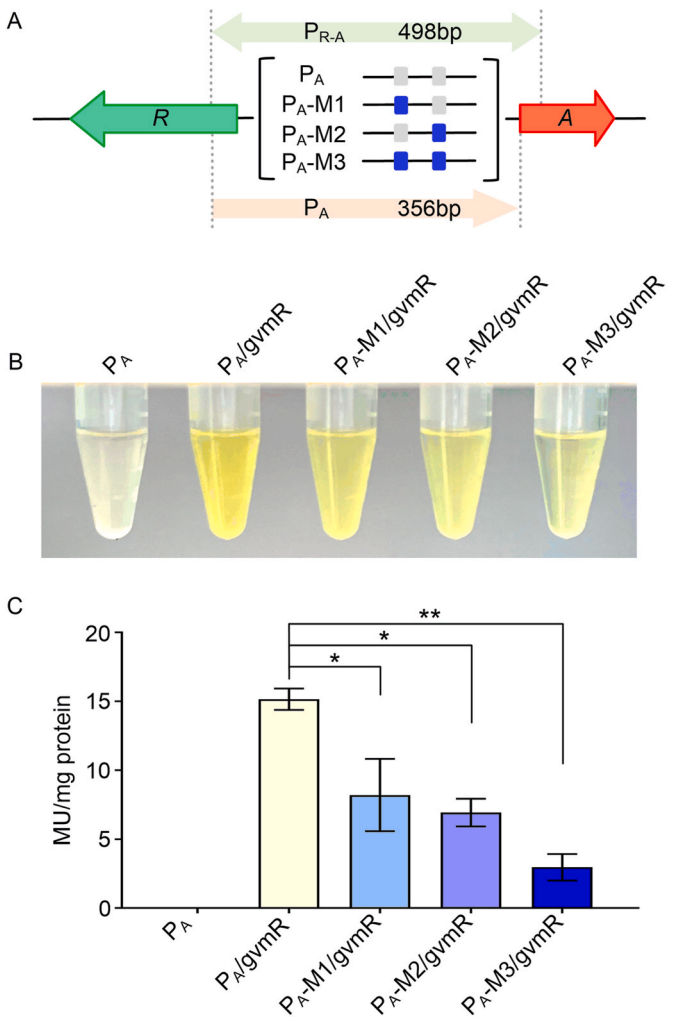

Fig. 5. Importance of the palindromic sequences in GvmR-mediated P_A activation. (A) Mutation diagram showing changes made to the two palindromic sequences in P_A. The gray box indicates wild-type palindromic sequences; the blue box indicates the site replaced by the *Nde*I or *Nhe*I restriction site. (B) GUS assays showing the effects of palindromic sequence mutation on GvmR-mediated P_A activation using p-nitrophenyl-β-D-glucuronide as a substrate. (C) Spectrophotometric assays measuring the effects of palindromic sequence mutation on GvmR-mediated P_A activation. P_A, ΔgvmR/$P_A$gusA; P_A/gvmR, ΔgvmR/$P_A$gusA::P_{hrdB}gvmR; P_A-M1/gvmR, ΔgvmR/P_A-M1gusA::P_{hrdB}gvmR; P_A-M2/gvmR, ΔgvmR/P_A-M2gusA::P_{hrdB}gvmR; P_A-M3/gvmR, ΔgvmR/P_A-M3gusA::P_{hrdB}gvmR.

P_{hrdB}gvmR, ΔgvmR/P_A-M2gusA::P_{hrdB}gvmR, ΔgvmR/P_A-M3gusA::P_{hrdB}gvmR, ΔgvmR/$P_A$gusA, all of which were cultivated in guvermectin fermentation medium for GUS activity measurements. In ΔgvmR/$P_A$gusA, P_A did not activate *gusA* expression. However, in pSET152:$P_A$gusA::P_{hrdB}gvmR, which showed constitutive GvmR expression, *gusA* transcription driven by P_A was easily detectable (Fig. 5B and C), further verifying direct P_A activation by GvmR. With constitutive GvmR expression, P_A mutations at sites I and II both caused significant decreases in GUS activity, with further decreases in GUS activity in the strain that had both sites mutated (Fig. 5B and C). These results clearly indicated that both 14-bp palindromic sequences (sites I and II) were necessary for GvmR activation.

3.6. Combined manipulation of gvmR and gvmR2 to improve guvermectin production

Overexpression of activator genes and deletion of repressor genes have proven effective in significantly improving the yield of NPs [29,30]. In guvermectin biosynthesis, *gvmR* functions as an activator, while *gvmR2* serves as a repressor. We sought to manipulate the two regulatory genes to optimize guvermectin production. Utilizing the integrative plasmid pSET152, we employed both the *gvmR* native promoter and the strong constitutive T7 RNA polymerase-T7 promoter system to modulate *gvmR* expression [20], and constructed three *gvmR*-overexpressing plasmids: pSET152:gvmR, pSET152:2gvmR (two copies of *gvmR* driven by its native promoter), and pSET152:pHT7gvmR (Fig. 6A). These recombinant plasmids and the control plasmid pSET152 were introduced into both NEAU6 and ΔgvmR2 to obtain six *gvmR* overexpression strains and two control strains, which were then analyzed for guvermectin production. The guvermectin titer in NEAU6/gvmR was comparable to that of NEAU6/pSET152. However, in NEAU6/2gvmR, guvermectin production was reduced (Fig. 6B). Guvermectin titers in ΔgvmR2/gvmR and ΔgvmR2/2gvmR were similar to that in ΔgvmR2/pSET152 (Fig. 6B). Notably, compared to the NEAU6 strain, the introduction of pSET152:pHT7gvmR into either NEAU6 or ΔgvmR2 strains markedly improved guvermectin production by 35.5 % and 125 %, reaching 855 mg L^{-1} and 1422 mg L^{-1}, respectively (Fig. 6B). These findings suggested that the constitutive T7 RNA polymerase-T7 promoter system had a beneficial effect on guvermectin production, but the *gvmR* native promoter had no discernible effect. Additionally, we assessed the biomass of NEAU6, NEAU6/pHT7gvmR, ΔgvmR2, and ΔgvmR2/pHT7gvmR. All four strains exhibited comparable growth rates and biomasses (Fig. 6C), indicating that the genetic manipulation of these two genes did not adversely influence bacterial growth.

4. Discussion

NP biosynthesis in *Streptomyces* is strictly controlled by an intricate cellular regulatory network. Transcriptional regulators form the framework of this network, controlling the initiation of NP production and the final titer through precise regulation of target gene transcription [9]. Comprehending the molecular mechanisms of these transcriptional regulators is essential for developing regulator-based rational strategies to attain NP overproduction [31]. In this study, we elucidated the molecular mechanisms of two LacI family transcription regulators, GvmR and GvmR2, in orchestrating guvermectin biosynthesis. As depicted in Fig. 7, GvmR functions as an activator of guvermectin biosynthesis by binding to the promoter regions of *gvmR*, *gvmA* and *O1*. Conversely, GvmR2 acts as a repressor, exerting its regulatory effect by binding to the same promoter regions as GvmR. Additionally, cross-regulation between *gvmR* and *gvmR2* was identified, indicating a complex interaction between these two regulators in coordinating guvermectin biosynthesis.

Overexpression of activator genes has been successfully employed to enhance the yield of various NPs like nikkomycin, toyocamycin, oxytetracycline, lincomycin *etc* [10,12,32]. However, the regulatory mechanisms governing NP biosynthesis are often intricate, and in some cases, overexpression of activators does not necessarily lead to increased yields and may even have detrimental effects. For example, the overexpression of the positive regulator *aveR* under the constitutive *ermEp** promoter resulted in a complete loss of avermectin production in *S. avermitilis* KA320 [33]. Similarly, the overexpression of the milbemycin CSR activator gene *milR* using the strong constitutive *hrdB* promoter produced a lower milbemycin level compared to the parental strain BC04 [19]. In this study, we observed an obvious decrease in guvermectin production upon overexpressing two copies of *gvmR* under its native promoter. This phenomenon warrants further examination. Notably, our exploration of the regulatory mechanisms of GvmR and GvmR2 and their cross-regulatory relationships may offer insights into these observations. While GvmR directly activates the guvermectin BGC, it also indirectly triggers *gvmR2*; overexpression of *gvmR* increases *gvmR2* expression level. Elevated *gvmR2* expression competes with GvmR to bind to the same promoters, thereby inhibiting the expression of the BGC and *gvmR* itself, leading to reduced guvermectin production.

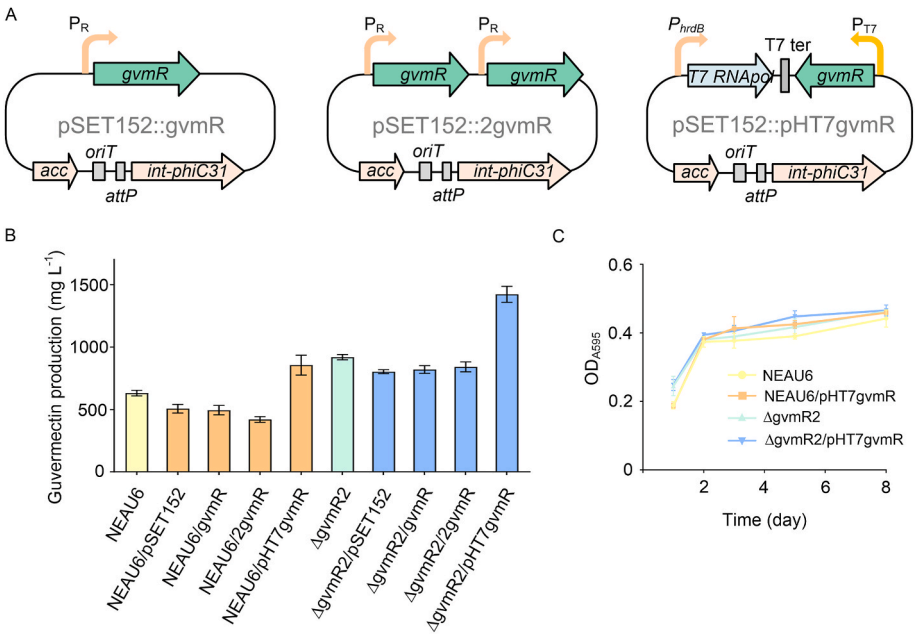

Fig. 6. Effects of *gvmR* overexpression on guvermectin production in NEAU6 and ΔgvmR2 strains. (A) Schematic diagrams of *gvmR* overexpression plasmids. (B) Guvermectin production in NEAU6 and its derivatives. (C) Growth curves of NEAU6 and its derivatives.

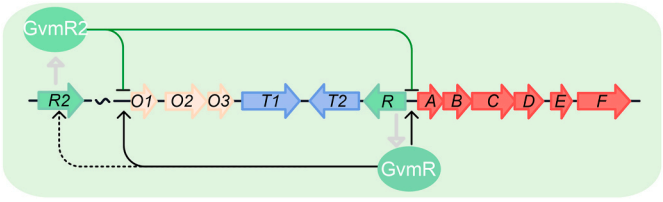

Fig. 7. Proposed model for the GvmR- and GvmR2-mediated regulation of guvermectin production in *S. caniferus* NEAU6. GvmR is essential for guvermectin production; it directly activates transcription of genes within the guvermectin BGC by binding to the promoter regions of *gvmR*, *gvmA*, and *O1*. Additionally, GvmR indirectly activates the transcription of *gvmR2*. Conversely, the cluster-adjacent regulator GvmR2 functions as a repressor of guvermectin biosynthesis by inhibiting transcription of the guvermectin BGC through competitive binding to the *gvmR*, *gvmA*, and *O1* promoter regions. The interplay between GvmR and GvmR2, along with their differential effects on guvermectin biosynthesis, provides new insights into how cluster-situated and cluster-adjacent regulators coordinate the production of natural products.

Interestingly, when the robust T7 RNA polymerase-T7 promoter system was employed to overexpress *gvmR* in the NEAU6 strain, guvermectin production was significantly enhanced. This suggests that the constitutive promoter may partially overcome the direct inhibitory effect of GvmR2 on *gvmR*, thereby strengthening the competitive activation of guvermectin biosynthesis genes by GvmR. Consequently, this promotes more efficient guvermectin production. Moreover, when GvmR was overexpressed in ΔgvmR2, guvermectin production in ΔgvmR2/gvmR and ΔgvmR2/2gvmR strains was similar to that in ΔgvmR2/pSET152. This indicates that, after removing the direct inhibition of GvmR2 on *gvmR*, *gvmR* overexpression under its native promoter no longer had a significant inhibitory effect on guvermectin production. Therefore, we propose that the feedback inhibition of *gvmR* expression by GvmR2 is an essential factor contributing to the suboptimal effect of *gvmR* manipulation on production. Additionally, the interplay between GvmR and GvmR2 highlights the necessity of optimizing the timing and strength of regulator expression to achieve high NP titers [34].

Our findings indicate that the introduction of integrated vectors pSET152 and pIJ10500 into NEAU6 strains negatively impacted guvermectin production. The insertion site of pSET152 into NEAU6 corresponds to *scn3880*, which encodes a cupin superfamily protein of 317 aa, including two Pirin domains. Pirin functions as an oxidative stress sensor and is implicated in a variety of biological processes [35]. In *Serratia marcescens*, Pirin regulates the conversion of pyruvate to acetyl-CoA, thereby directing pyruvate metabolism toward either the TCA cycle or fermentation pathways [36]. The inactivation of *scn3880* may disturb primary metabolism processes in NEAU6 strains, subsequently affecting guvermectin biosynthesis. The insertion site of pIJ10500 in NEAU6 was *scn4771*, which encodes a putative integral membrane protein of 105 aa, conserved across *Streptomyces* species. SCN4771 contains an E1-E2 ATPase domain that is likely involved in cation transport. Disruption of the *scn4771* ortholog, *sco4848*, has been shown to delay spore germination in *Streptomyces coelicolor*. However, the precise role of *scn4771* orthologs in secondary metabolism remains largely unexplored [37]. We hypothesize that SCN4771, as a membrane protein component, may influence guvermectin production by modulating the cellular response to environmental cues or by interacting with unknown signaling pathways, which requires further investigation.

In this study, we have elucidated a complex mini-regulatory pathway encompassing two LacI-family regulators, GvmR and GvmR2, which are pivotal in modulating guvermectin biosynthesis. This detailed understanding of their regulatory mechanisms offers valuable theoretical insights into optimizing guvermectin yield. The engineered guvermectin high-titer strain, ΔgvmR2/pHT7gvmR, designed in this work, holds promise as a novel parental strain for future genetic engineering efforts to develop superior guvermectin producers.

CRediT authorship contribution statement

Haoran Shi: Writing – original draft, Project administration, Methodology, Investigation. **Jiabin Wang:** Writing – original draft, Project administration, Methodology, Investigation. **Shanshan Li:** Visualization, Investigation, Funding acquisition. **Chongxi Liu:** Visualization, Investigation. **Lei Li:** Visualization, Investigation. **Zhuoxu Dong:** Visualization, Investigation. **Lan Ye:** Visualization, Investigation. **Xiangjing Wang:** Visualization, Investigation. **Yanyan Zhang:** Writing – review & editing, Writing – original draft, Project administration, Methodology, Funding acquisition, Formal analysis, Conceptualization. **Wensheng**

Xiang: Writing – review & editing, Supervision, Resources, Conceptualization.

Declaration of competing interest

The authors declare that they have no known competing financial interests or personal relationships that could have appeared to influence the work reported in this paper.

Acknowledgments

This work was supported by the National Key Research and Development Program of China (2022YFD1700205), and the Agricultural Sciences and Technology Innovation Program (CAAS-CSCB-202401). We would like to thank Professor Mervyn Bibb (John Innes Centre, Norwich, UK) for providing *S. coelicolor* M1146, and Professor Mark Buttner (John Innes Centre, Norwich, UK) for providing pIJ10500.

Appendix A. Supplementary data

Supplementary data to this article can be found online at https://doi.org/10.1016/j.synbio.2024.11.001.

References

[1] Yuntsen H, Yonehara H, Ui H. Studies on a new antibiotic, angustmycin. I. J Antibiot (Tokyo) 1954;7:113–5.
[2] Yuntsen H, Ohkuma K, Ishii Y, Yonehara H. Studies on angustmycin. III. J Antibiot (Tokyo) 1956;9:195–201.
[3] Sugimori T, Suhadolnik RJ. The biosynthesis of psicofuranine. J Am Chem Soc 1965;87:1136–7. https://doi.org/10.1021/ja01083a038.
[4] Liu C, Bai L, Cao P, Li S, Huang S-X, Wang J, et al. Novel plant growth regulator guvermectin from plant growth-promoting rhizobacteria boosts biomass and grain yield in rice. J Agric Food Chem 2022;70:16229–40. https://doi.org/10.1021/acs.jafc.2c07072.
[5] Liu C, Zhang M, Li L, Wang X, Li S, Xiang W. Development and application of the novel plant growth regulator guvermectin: a perspective. J Agric Food Chem 2024;72:8365–71. https://doi.org/10.1021/acs.jafc.3c09704.
[6] Yu L, Zhou W, She Y, Ma H, Cai Y-S, Jiang M, et al. Efficient biosynthesis of nucleoside cytokinin angustmycin A containing an unusual sugar system. Nat Commun 2021;12:6633. https://doi.org/10.1038/s41467-021-26928-y.
[7] Shiraishi T, Xia J, Kato T, Kuzuyama T. Biosynthesis of the nucleoside antibiotic angustmycins: identification and characterization of the biosynthetic gene cluster reveal unprecedented dehydratase required for exo-glycal formation. J Antibiot (Tokyo) 2021;74:830–3. https://doi.org/10.1038/s41429-021-00466-7.
[8] Liu C, Wang Z, Chen Y, Yan Y, Li L, Wang Y-J, et al. Guvermectin biosynthesis revealing the key role of a phosphoribohydrolase and structural insight into the active glutamate of a noncanonical adenine phosphoribosyltransferase. ACS Chem Biol 2023;18:102–11. https://doi.org/10.1021/acschembio.2c00739.
[9] Liu G, Chater KF, Chandra G, Niu G, Tan H. Molecular regulation of antibiotic biosynthesis in *streptomyces*. Microbiol Mol Biol Rev 2013;77:112–43. https://doi.org/10.1128/MMBR.00054-12.
[10] Wei J, He L, Niu G. Regulation of antibiotic biosynthesis in actinomycetes: perspectives and challenges. Synth Syst Biotechnol 2018;3:229–35. https://doi.org/10.1016/j.synbio.2018.10.005.
[11] Romero-Rodríguez A, Robledo-Casados I, Sánchez S. An overview on transcriptional regulators in *Streptomyces*. Biochim Biophys Acta 2015;1849:1017–39. https://doi.org/10.1016/j.bbagrm.2015.06.007.
[12] Bu Q, Li Y, Xie H, Li J, Lv Z, Su Y, et al. Rational engineering strategies for achieving high-yield, high-quality and high-stability of natural product production in actinomycetes. Metab Eng 2021;67:198–215. https://doi.org/10.1016/j.ymben.2021.06.003.
[13] Li Y, Tan H. Biosynthesis and molecular regulation of secondary metabolites in microorganisms. Sci China Life Sci 2017;60:935–8. https://doi.org/10.1007/s11427-017-9115-x.
[14] Gomez-Escribano JP, Bibb MJ. Engineering *Streptomyces coelicolor* for heterologous expression of secondary metabolite gene clusters. Microb Biotechnol 2011;4:207–15. https://doi.org/10.1111/j.1751-7915.2010.00219.x.
[15] Kieser T, Bibb MJ, Chater KF, Butter M, Hopwood D, Bittner ML, et al. Practical Streptomyces genetics: a laboratory manual. 2000.
[16] Bierman M, Logan R, O'Brien K, Seno ET, Rao RN, Schoner BE. Plasmid cloning vectors for the conjugal transfer of DNA from Escherichia coli to *Streptomyces spp*. Gene 1992;116:43–9. https://doi.org/10.1016/0378-1119(92)90627-2.
[17] Kuhstoss S, Richardson MA, Rao RN. Plasmid cloning vectors that integrate site-specifically in *Streptomyces spp*. Gene 1991;97:143–6. https://doi.org/10.1016/0378-1119(91)90022-4.
[18] Ikeda H, Kotaki H, Tanaka H, Omura S. Involvement of glucose catabolism in avermectin production by *Streptomyces avermitilis*. Antimicrob Agents Chemother 1988;32:282–4. https://doi.org/10.1128/AAC.32.2.282.
[19] Zhang Y, He H, Liu H, Wang H, Wang X, Xiang W. Characterization of a pathway-specific activator of milbemycin biosynthesis and improved milbemycin production by its overexpression in *Streptomyces bingchenggensis*. Microb Cell Factories 2016;15:152. https://doi.org/10.1186/s12934-016-0552-1.
[20] Wei J, Tian J, Pan G, Xie J, Bao J, Zhou Z. Development and application of a T7 RNA polymerase-dependent expression system for antibiotic production improvement in *Streptomyces*. Biotechnol Lett 2017;39:857–64. https://doi.org/10.1007/s10529-017-2309-2.
[21] Zhang Y, Pan G, Zou Z, Fan K, Yang K, Tan H. JadR*-mediated feed-forward regulation of cofactor supply in jadomycin biosynthesis. Mol Microbiol 2013;90:884–97. https://doi.org/10.1111/mmi.12406.
[22] Li C, He H, Wang J, Liu H, Wang H, Zhu Y, et al. Characterization of a LAL-type regulator NemR in nemadectin biosynthesis and its application for increasing nemadectin production in *Streptomyces cyaneogriseus*. Sci China Life Sci 2019;62:394–405. https://doi.org/10.1007/s11427-018-9442-9.
[23] Myronovskyi M, Welle E, Fedorenko V, Luzhetskyy A. Beta-glucuronidase as a sensitive and versatile reporter in actinomycetes. Appl Environ Microbiol 2011;77:5370–83. https://doi.org/10.1128/AEM.00434-11.
[24] Sherwood EJ, Bibb MJ. The antibiotic planosporicin coordinates its own production in the actinomycete *Planomonospora alba*. Proc Natl Acad Sci U S A 2013;110:E2500–9. https://doi.org/10.1073/pnas.1305392110.
[25] Zhao Y, Xiang S, Dai X, Yang K. A simplified diphenylamine colorimetric method for growth quantification. Appl Microbiol Biotechnol 2013;97:5069–77. https://doi.org/10.1007/s00253-013-4893-y.
[26] Matilla MA, Velando F, Martín-Mora D, Monteagudo-Cascales E, Krell T. A catalogue of signal molecules that interact with sensor kinases, chemoreceptors and transcriptional regulators. FEMS Microbiol Rev 2022;46. https://doi.org/10.1093/femsre/fuab043.
[27] Schumacher MA, Choi KY, Zalkin H, Brennan RG. Crystal structure of LacI member, PurR, bound to DNA: minor groove binding by alpha helices. Science 1994;266:763–70. https://doi.org/10.1126/science.7973627.
[28] Swint-Kruse L, Matthews KS. Allostery in the LacI/GalR family: variations on a theme. Curr Opin Microbiol 2009;12:129–37. https://doi.org/10.1016/j.mib.2009.01.009.
[29] Li L, Zhao Y, Ruan L, Yang S, Ge M, Jiang W, et al. A stepwise increase in pristinamycin II biosynthesis by *Streptomyces pristinaespiralis* through combinatorial metabolic engineering. Metab Eng 2015;29. https://doi.org/10.1016/J.YMBEN.2015.02.001.
[30] Zhou Q, Ning S, Luo Y. Coordinated regulation for nature products discovery and overproduction in *Streptomyces*. Synth Syst Biotechnol 2020;5:49–58. https://doi.org/10.1016/j.synbio.2020.04.002.
[31] Ye L, Zhang Y, Li S, He H, Ai G, Wang X, et al. Transcriptome-guided identification of a four-component system, SbrH1-R, that modulates milbemycin biosynthesis by influencing gene cluster expression, precursor supply, and antibiotic efflux. Synth Syst Biotechnol 2022;7:705–17. https://doi.org/10.1016/j.synbio.2022.02.003.
[32] Yin S, Wang W, Wang X, Zhu Y, Jia X, Li S, et al. Identification of a cluster-situated activator of oxytetracycline biosynthesis and manipulation of its expression for improved oxytetracycline production in *Streptomyces rimosus*. Microb Cell Factories 2015;14:46. https://doi.org/10.1186/s12934-015-0231-7.
[33] Kitani S, Ikeda H, Sakamoto T, Noguchi S, Nihira T. Characterization of a regulatory gene, aveR, for the biosynthesis of avermectin in *Streptomyces avermitilis*. Appl Microbiol Biotechnol 2009;82:1089–96. https://doi.org/10.1007/s00253-008-1850-2.
[34] Li S, Wang J, Xiang W, Yang K, Li Z, Wang W. An autoregulated fine-tuning strategy for titer improvement of secondary metabolites using native promoters in *streptomyces*. ACS Synth Biol 2018;7:522–30. https://doi.org/10.1021/acssynbio.7b00318.
[35] Perez Dominguez F, Carrillo Beltrán D, Blanco R, Muñoz JP, León Cruz G, Corvalan AH, et al. Role of Pirin, an oxidative stress sensor protein, in *epithelial carcinogenesis*. Biology 2021;10. https://doi.org/10.3390/biology10020116.
[36] Soo P, Horng Y, Lai M, Wei J, Hsieh S, Chang Y, et al. Pirin regulates pyruvate catabolism by interacting with the pyruvate dehydrogenase E1 subunit and modulating pyruvate dehydrogenase activity. J Bacteriol 2007;189:109–18. https://doi.org/10.1128/JB.00710-06.
[37] Gonzalez Quiñonez N, López García MT, Yagüe P, Rioseras B, Pisciotta A, Alduina R, et al. New ΦBT1 site-specific integrative vectors with neutral phenotype in *Streptomyces*. Appl Microbiol Biotechnol 2016;100:2797–808. https://doi.org/10.1007/s00253-015-7271-0.